

# STUDIES OF $(p,\pi)$ AND $(p,2\pi)$ REACTIONS ON THE INDIANA COOLER RING USING RECOIL DETECTION\*

H. NANN

for the CE06 Collaboration

R.E. Segel, F.-J. Chen, P. Heimberg and Z. Yu,  
Northwestern University, Evanston, IL 60201, USA;

J.D. Brown and E. Jacobsen,  
Princeton University, Princeton, NJ 08540, USA;

J. Homolka and R. Schneider,  
Physik Department, Technische Universität München, Germany;

A. Zhuravlev and A. Kurepin,  
Institute for Nuclear Research, Moscow, Russia;

G. Hardie and P. Pancella,  
Western Michigan University, Kalamazoo, MI 49008, USA;

K.E. Rehm,  
Argonne National Laboratory, Argonne, IL 60439, USA;  
R.D. Bent, J. Blomgren, H. Nann, T. Rinckel, M. Saber and C. Sun,  
Indiana University Cyclotron Facility, Bloomington, IN 47408, USA.

*(Received July 7, 1993)*

Studies of the  $^{12}\text{C}(p,\pi)$  and  $^{12}\text{C}(p,2\pi)$  reactions on the Indiana Cooler Ring using recoil ion detection will be described. This method allows to simultaneously measure the cross sections for pion production in the different isospin channels with the same target and detection system. The use of very thin internal targets in a storage ring environment greatly reduces the energy resolution limits set by the energy loss of the recoiling ions in the target.

PACS numbers: 13.75. Gx

---

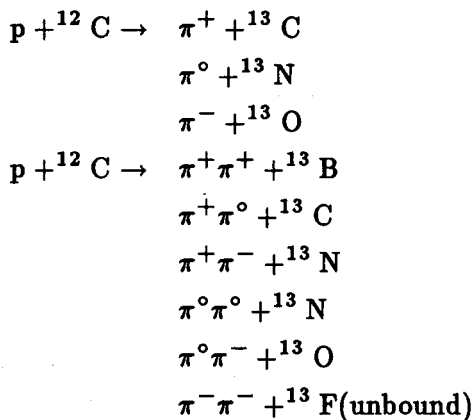
\* Presented at the Meson-Nucleus Interactions Conference, Cracow, Poland, May 14-19, 1993.

## 1. Introduction

The study of proton induced pion production has been a major area of interest at IUCF. While it is fairly easy to measure spectra of charged pions with good energy resolution using magnetic spectrometers, it is very difficult, if not impossible, to obtain spectra of the neutral pion with similar accuracy. Thus a technique using recoil ion detection for studying nuclear reactions with high-momentum transfer has been developed at IUCF for several years [1].

The recoil detection technique provides an extremely efficient method for obtaining  $(p,\pi)$  and  $(p,2\pi)$  data, because, due to the high momentum transfer, the recoil ions are emitted into a small forward cone, and hence a small detector array in the laboratory covers a large center-of-mass angular range. In many cases, the magnetic rigidity of the recoil ions is much smaller than that of the projectile, thereby facilitating the magnetic separation of the recoil ions from the beam.

Furthermore, it is possible to simultaneously measure single and double pion production cross sections for different isospin channels with the same beam, same target, and same detection system. For example, for protons on a carbon target, the following  $(p,\pi)$  and  $(p,2\pi)$  reactions can occur:



With the recoil detection method, all of the mass 13 recoils are detected at the same time (except for  ${}^{13}\text{F}$  which is unbound). This makes it an extremely valuable tool for obtaining reliable branching ratios for production of the various isospin final states.

## 2. Single Pion Production

Despite extensive experimental and theoretical investigations of single pion production in a proton-nucleus collision, the process is still not well

understood. Models developed so far have been successful in explaining only small fragments of the available data [2, 3, 4].

There are essentially two different models which have been used to describe the  $(p, \pi)$  cross section. In the one-nucleon mechanism (ONM), the pion is produced directly from the projectile in a stripping or bremsstrahlung-like process (Fig. 1(a)). Here the large momentum transfer ( $\geq 480 \text{ MeV}/c$ ) is taken up by a single-nucleon wave function. However, the high momentum components of typical nuclear wave functions are very small and also poorly determined. Many aspects of the data were not explained by the SNM, *e.g.* the strong excitation of two particle-one hole configuration and more complicated core excited states or the excitation of single-neutron final states in the  $(p, \pi^+)$  reaction.

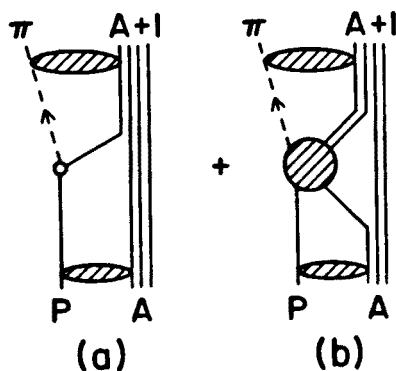


Fig. 1. Schematic diagrams of one-nucleon (a) and two-nucleon (b) mechanism for proton induced pion production.

Another model is the two-nucleon mechanism (TNM), in which the pion is produced in a collision between the incident proton and a target nucleon (Fig. 1(b)). Here the large momentum transfer is absorbed by two nucleons, resulting in the excitation of two particle-one hole and more complicated final states. Since in the  $(p, \pi^-)$  reaction the total nuclear charge is increased by two while gaining only one nucleon, this reaction must explicitly involve at least two nucleons.

The  $^{12}\text{C}(p, \pi^+)^{13}\text{C}$  reaction has been studied by several groups using magnetic spectrometers to measure the pion spectra [5, 6]. Since a direct measurement of  $\pi^0$ 's from the  $^{12}\text{C}(p, \pi^0)^{13}\text{N}$  is very difficult, Homolka *et al.* [7] detected the recoiling  $^{13}\text{N}$  ions with high efficiency in a magnetic spectrometer having a moderate solid angle. Since  $^{13}\text{N}$  has no bound excited states, only one  $^{13}\text{N}$  recoil ion group has had to be considered. Differential cross sections were measured at 153.5, 166.1, 186.0, and 204.0 MeV

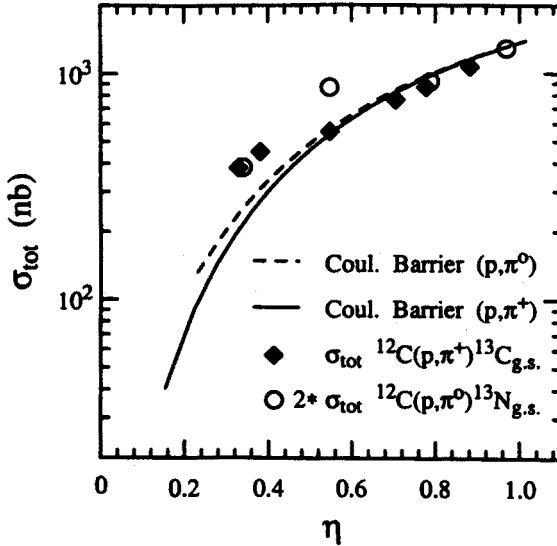


Fig. 2. Total cross section, as a function of scaled pion momentum, for the  $^{12}\text{C}(p, \pi^+)^{13}\text{C}_{g.s.}$  and  $^{12}\text{C}(p, \pi^0)^{13}\text{N}_{g.s.}$  reactions. The  $(p, \pi^0)$  cross sections have been multiplied by 2.

bombarding energy and compared to  $(p, \pi^+)$  ground state transition cross sections at similar values of the reduced pion momentum  $\eta$  in the c.m. system. The total cross sections for the two mirror  $(p, \pi)$  reactions are plotted in Fig. 2. The  $\pi^0$  data have been multiplied by 2 to take into account isospin invariance. Also plotted in Fig. 2 are results from R-matrix calculations for the two reactions. A notable feature is that for  $\eta < 0.4$  both the  $(p, \pi^0)$  and  $(p, \pi^+)$  cross sections are substantially larger than the R-matrix predictions implying an energy dependence of the R-matrix elements. At 154, 186, and 204 MeV, the ratio  $\sigma(p, \pi^+)/\sigma(p, \pi^0)$  is 2 as expected, but at 166 MeV this ratio rises to 3. The reason for this anomalous value is not apparent. One explanation might be that this anomalous value is caused by the opening of the  $^{12}\text{C}(p, \pi^-)^{13}\text{O}$  channel, the threshold of which lies at 168.9 MeV.

### 3. Double pion production

Recent theoretical studies of the  $(\pi, 2\pi)$  reaction indicate that this reaction provides a natural testing ground of nonlinear pion-nucleon dynamics and the underlying chiral Lagrangians. The reaction mechanism has been studied in detail by Oset and Vicente-Vacas [8]. They claim that, close to threshold, only two Feynman diagrams, the so-called pion-pole term and the contact term (top of Fig. 3), will contribute to the cross section.

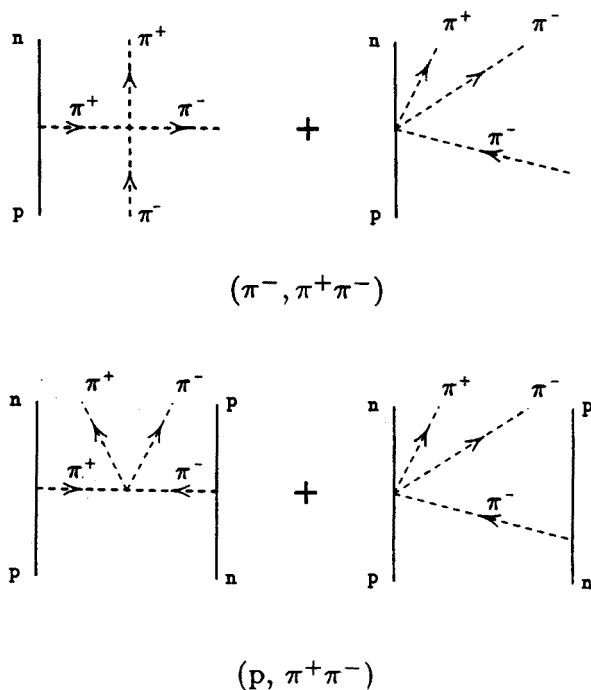


Fig. 3. Dominant Feynman diagrams for the  $(\pi, 2\pi)$  and  $(p, 2\pi)$  reactions close to threshold.

While there have been no theoretical calculations of the  $(p, 2\pi)$  reaction comparable to those of Oset and Vicente-Vacas for the  $(\pi, 2\pi)$  reaction, it is expected [9], by analogy, that the two dominant diagrams for the  $(p, 2\pi)$  reaction near threshold will be those shown at the bottom of Fig. 3. In this picture the first pion is produced via an  $NN \rightarrow NN\pi$  reaction and the second pion is knocked out of the nuclear pion cloud by the first pion. This gives a simple model for the  $(p, 2\pi)$  reaction near threshold that should provide a good starting point for theoretical calculations. To our knowledge, there are no  $A(p, 2\pi)A+1$  data near threshold.

The isospin selectivity of the  $(p, 2\pi)$  reactions allows one to separate the two non-linear terms. For example, the  $^{12}\text{C}(p, \pi^+ \pi^+)^{13}\text{B}$  reaction is dominated by the  $4\pi$  diagram at threshold, whereas the  $3\pi$  and  $4\pi$  diagrams both contribute to the  $^{12}\text{C}(p, \pi^+ \pi^-)^{13}\text{C}$  reaction. A measurement of the ratio of cross sections for producing  $^{13}\text{B}$  and  $^{13}\text{C}$  recoils near threshold would yield information about the relative importance of the  $3\pi$  and  $4\pi$  production mechanisms.

An additional motivation for double pion production is a recent specu-

lation by Schuck *et al.* [10]. They conjecture that two-pion clusters may be stabilized in nuclear matter due to self-energy effects resulting from nucleon-hole and delta-hole excitations. They suggest that the  $(p, 2\pi)$  reaction is a promising tool for looking for evidence of a bound or quasi-bound  $\pi\pi$ -state in nuclear matter. The width of such a  $\pi\pi$ -state is predicted to be less than 30 MeV. Its experimental signature might be an enhancement in the cross section close to threshold.

#### 4. Experiment

The experimental apparatus for measuring the  $^{12}\text{C}(p, \pi)$  and  $^{12}\text{C}(p, 2\pi)$  cross sections near threshold with the recoil detection technique was mounted in the T-section of the IUCF Cooler Ring. A close-up is shown in Fig. 4. The magnet in the Cooler Ring that bends the primary beam by  $6^\circ$  separates the recoil ions from the beam and sweeps them into a detection system that consists of a parallel grid avalanche counter (PGAC), a proportional counter (PC), and an array of 24 silicon microstrip detectors.

#### *CE-06 Detector Stack*

PGAC:	$X, Y$
PC:	$DE, Y$
SI:	$E, X$
PGAC-SI:	TOF
PC-SI:	Recoil identification
Raytracing:	$P/Q, \theta$

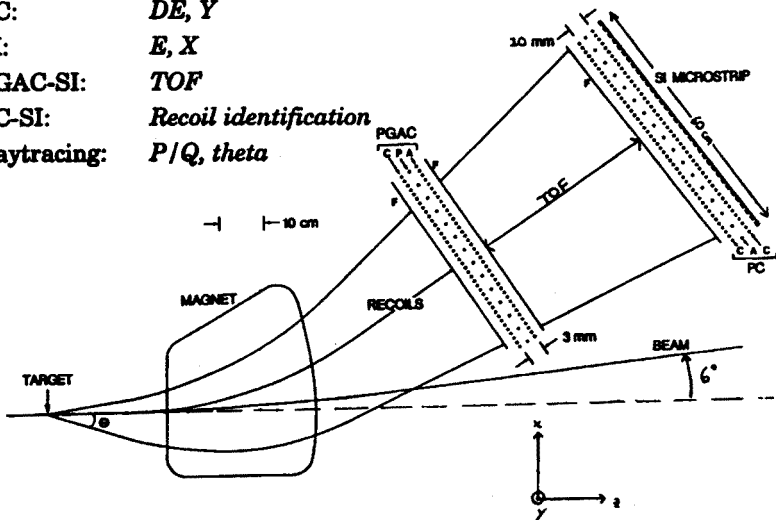


Fig. 4. Schematic view of the recoil ion detection system.

The PGAC measures the time and  $(x, y)$ -position of the recoil ions emerging from the " $6^\circ$ -magnet". It has 0.9 micron thick entrance and exit foils, a position resolution of about 1 mm in both dimensions and a time resolution of 0.65 ns. The PC measures the energy loss  $dE/dx$  of the recoil

ions and the  $y$ -position with a spatial resolution of about 4 mm. The recoil ions are stopped in an array of Si microstrip detectors, which measure the total energy and  $x$  position. They are mounted in the same housing as the PC. Time-of-flight (TOF) of the recoil ions is measured between the PGAC and the Si detectors which are about 64 cm apart.

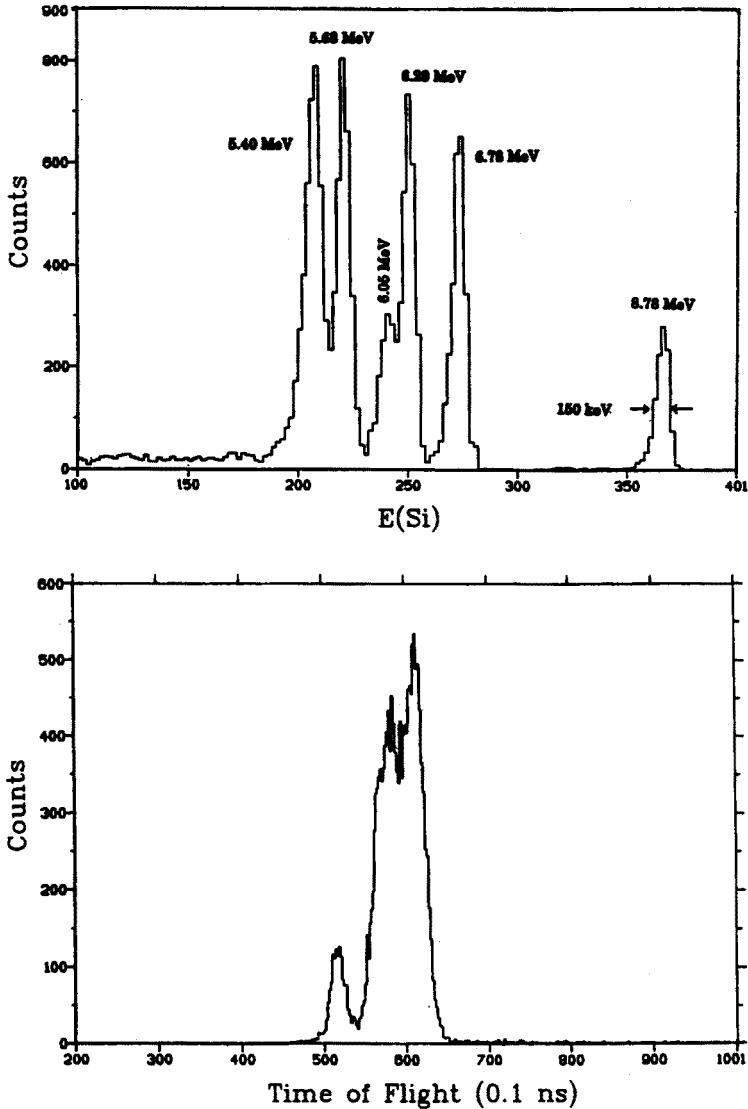


Fig. 5. Energy (top) and time-of-flight (bottom) spectrum of  $\alpha$  particles from a  $^{228}\text{Th}$  source measured with the Si microstrip detectors.

Each Si detector has 50 ion implanted strips of 1mm width which are contacted at the front of the detector. The energy and time signal is read out from the back contact of the detector. Using only a resistor network and charge division to read out the strips to get the position information would lead to an energy signal with poor risetime and thus not allowing fast timing. Therefore it is necessary to add a small capacitive load to ground to each strip. However, this RC chain would add considerable noise to the position signal thus not allowing to measure recoil ions with less than 1 MeV. This problem was solved by inserting a discriminator between each strip and the resistor chain. In this way the noise contribution from the resistor chain and the capacitive loads of all the other strips to the position signal was avoided.

The Si microstrip detectors had 1 mm position, 0.80 ns time and 160 keV energy resolutions. The top half of Fig. 5 shows the energy spectrum of  $\alpha$  particles from a  $^{228}\text{Th}$  source and the bottom half the corresponding TOF spectrum between the PGAC and the Si detectors. The overall TOF resolution is about 1.4 ns.

The "6°-magnet" gives a rough measurement of the rigidity  $R = p/Q = Mv/Q$  of the recoil ion, where  $p$  is its momentum,  $Q$  its atomic charge,  $M$  its atomic mass and  $v$  its velocity. The momentum per unit charge,  $p/Q$ , and the emission angle,  $\theta$ , of the recoil ions can be determined from the two  $(x, y)$  positions by ray-tracing back through the "6°-magnet" to the target position. By dividing  $p/Q$  by the recoil ion velocity  $v$ , determined from the TOF between the PGAC and the Si detectors,  $M/Q$  can be determined.

## 5. Measurements and data analysis

The first experiments of the  $^{12}\text{C}(p, \pi)$  and  $^{12}\text{C}(p, 2\pi)$  reactions were carried out in November/December 1992 and February 1993 at bombarding energies of 166, 200, 250, 290, 330, and 350 MeV using carbon fiber and foil skimmer targets. Luminosities of several  $\times 10^{29} \text{cm}^{-2} \text{s}^{-1}$  were achieved.

When the same final recoil ion is produced by either the  $^{12}\text{C}(p, \pi)$  or the  $^{12}\text{C}(p, 2\pi)$  reaction, the difference in kinematics of the two reactions can be used to separate events from single and double pion production. Recoil ions from single pion production lie on an ellipse (or a series of closely spaced ellipses) in the momentum-angle plane that is far outside the region in which the recoils from double pion production are confined. This is depicted in Fig. 6 for the  $^{12}\text{C}(p, \pi^+)^{13}\text{C}$  and  $^{12}\text{C}(p, \pi^+ \pi^-)^{13}\text{C}$  reactions at 330 MeV bombarding energy. Also shown are the acceptance limits of the recoil ion detection system used.

Analysis is in progress to determine the  $^{12}\text{C}(p, \pi^0)^{13}\text{N}$  differential cross section, check the  $^{12}\text{C}(p, \pi^0/\pi^+)$  cross section anomaly described above, and search for  $(p, 2\pi)$  events at the two highest bombarding energies.



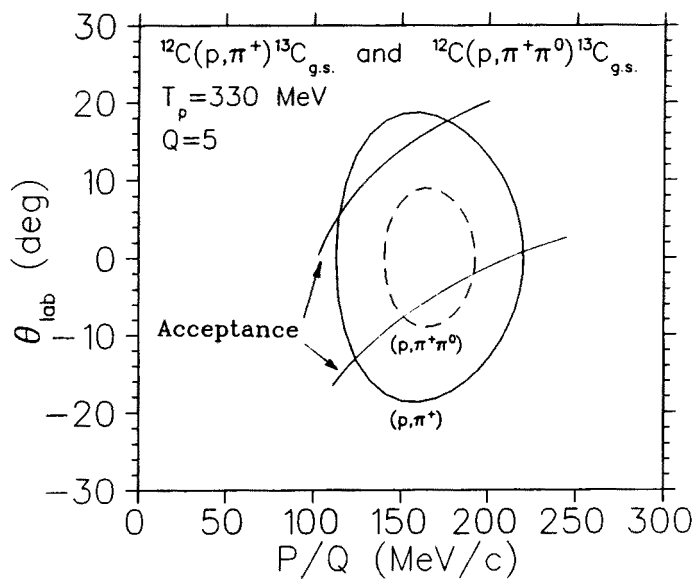


Fig. 6. Angle vs momentum of the recoil ions from the  $(p, \pi^+)$  and  $(p, \pi^+ \pi^-)$  reactions on  $^{12}\text{C}$  at 330 MeV bombarding energy.

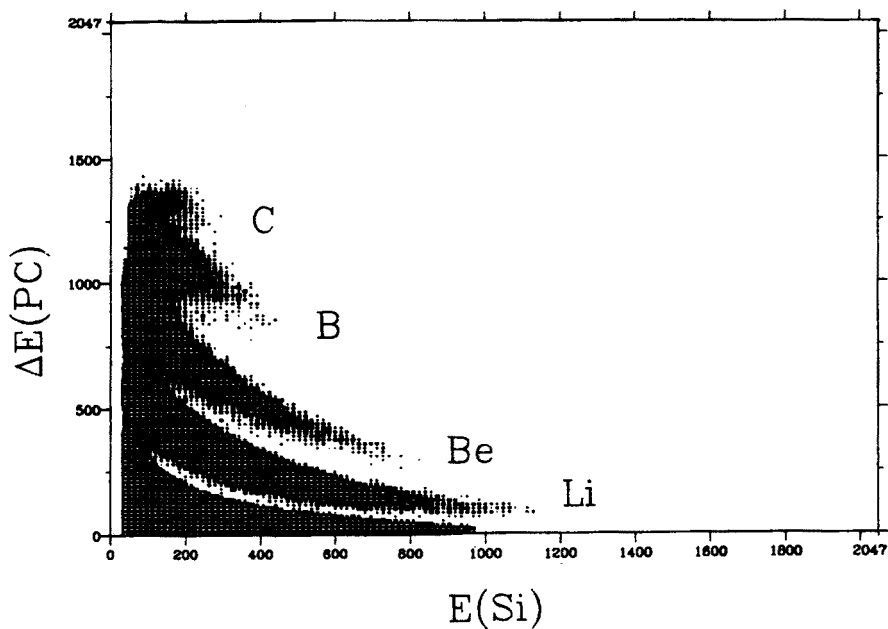


Fig. 7. Nuclear charge separation

Figs 7–9 show results of off-line analysis of some of the 330 MeV  $p+^{12}\text{C}$  data taken in the February 1993 run:

Fig. 7 shows  $\Delta E(PC)$  vs  $E(\text{Si})$ . The data, primarily light recoils (He, Li, Be, and B) from spallation reactions, are corrected for overall and differential gain variations of the 25 individual  $PC$  wires. The nuclear charge,  $Z$ , separation is quite good.

Fig. 8 shows a two-dimensional histogram of the atomic mass as determined from  $E/v^2$  and  $R/v$  for different atomic charges  $Q$  with  $Z = 6$  condition on the  $\Delta E(PC)$  vs  $E(\text{Si})$  spectrum. The different carbon isotopes are fairly well separated.

Fig. 9 shows the angle of emission ( $\Theta_{\text{lab}}$ ) vs magnetic rigidity ( $p/Q$ ) determined by backward ray tracing for  $^{13}\text{C}$  recoil ions in the  $Q=5$  charge state from the  $^{12}\text{C}(p,\pi^+)^{13}\text{C}$  and  $^{12}\text{C}(p,\pi^+\pi^0)^{13}\text{C}$  reactions. The  $^{13}\text{C}$  recoil ions are confined to at  $19^\circ$  cone about the beam axis. The diagonal cuts in upper and lower parts are due to the detector acceptance. The right hand portion of the  $(p/Q, \Theta_{\text{lab}})$  ellipse is missing, since the corresponding high-rigidity recoil ions are not bent enough by the  $6^\circ$  magnet to hit the detectors. Several events from the  $^{12}\text{C}(p,\pi^+\pi^0)^{13}\text{C}$  reaction have been identified.

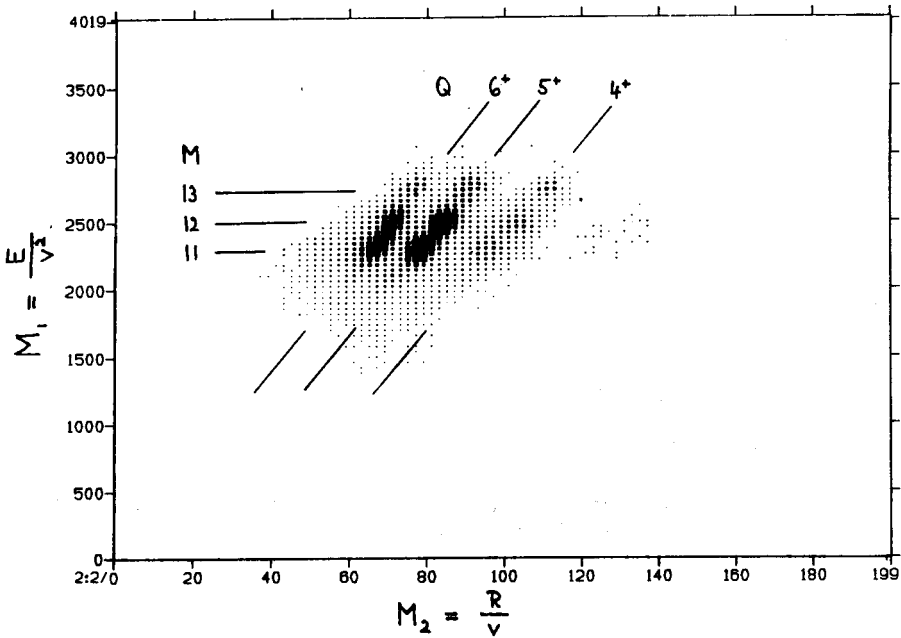


Fig. 8. Mass and atomic charge separation for  $Z = 6$

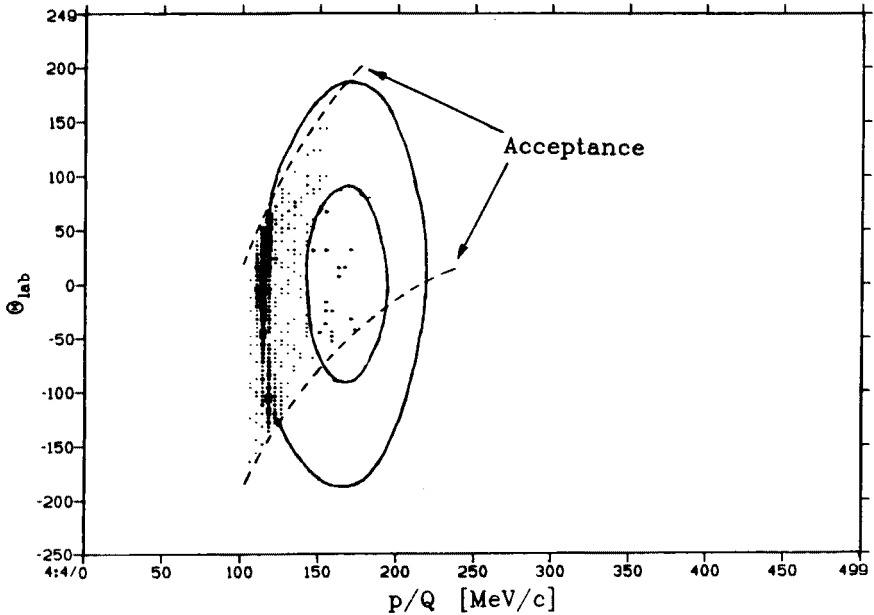


Fig. 9. Laboratory angle of emission vs magnetic rigidity determined by backward ray tracing.

## 6. Outlook

Experiments planned for the future include: measurements of the cross section and isospin selectivity of the  $(p, 2\pi)$  reaction near threshold to obtain information about non-linear terms (to third and fourth order in the pion field) in the  $\pi N$  interaction [9]; a search for evidence of a possible quasi-bound two-pion state in nuclei [10]; a search for corroborative evidence of possible resonant two-pion production near 350 MeV bombarding energy [11, 12]; and studies of the  $(\bar{p}, \gamma)$  reaction with polarized beam. In addition, the possibility of using the detector stack to measure recoils accompanying pion production by heavy ions is being investigated.

This work is supported in part by the U.S. National Science Foundation, the U.S. Department of Energy and the German Bundesministerium für Forschung und Technologie.

## REFERENCES

- [1] W. Schott *et al.*, *Phys. Rev.* **C34**, 1406 (1986); J. Homolka *et al.*, *Nucl. Instr. Meth.* **A260**, 418 (1987).
- [2] B. Hoistad, in *Adv. in Nucl. Phys.*, ed. J. Negele and E. Vogt, Plenum, New York, 1979, vol. 11, p. 135.
- [3] D.F. Measday, G.A. Miller, *Ann. Rev. Nucl. Part. Sci.* **29**, 121 (1979).
- [4] H.W. Fearing, in *Progr. Part. Nucl. Phys.*, ed. D.H. Wilkinson, Pergamon, Oxford, 1981, vol. 7, p. 113.
- [5] F. Soga *et al.*, *Phys. Rev.* **C24**, 570 (1981).
- [6] M.C. Green, Internal Report No. 83-31, Indiana University, Bloomington, Indiana, 1983 (unpublished).
- [7] J. Homolka *et al.*, *Phys. Rev.* **C36**, 2686 (1988).
- [8] E. Oset, M.J. Vicente-Vacas, *Nucl. Phys.* **A446**, 584 (1985).
- [9] M. Dillig, private communication.
- [10] P. Schuck, W. Nörenberg, G. Chanfray, *Z. Phys. A-Atomic Nuclei* **330**, 119 (1988).
- [11] V.A. Krasnov *et al.*, *Phys. Lett.* **108B**, 11 (1982).
- [12] J. Julien *et al.*, *Phys. Lett.* **142B**, 340 (1984).